Winchcombe: An example of rapid terrestrial alteration of a CM chondrite

Laura E. JENKINS [1]*, Martin R. LEE [1], Luke DALY [1,2,3], Ashley J. KING [4],
Cameron J. FLOYD[1], Pierre-Etienne MARTIN[1], Natasha V. ALMEIDA[4], and Matthew J. GENGE [5]

[1]School of Geographical and Earth Sciences, The University of Glasgow, Glasgow G12 8RZ, UK
[2]Space Science and Technology Centre, School of Earth and Planetary Sciences, Curtin University, Perth, Western Australia 6845, Australia
[3]Australian Centre for Microscopy and Microanalysis, The University of Sydney, Sydney, New South Wales 2006, Australia
[4]Planetary Materials Group, Natural History Museum, London SW7 5BD, UK
[5]Department of Earth Science and Engineering, Imperial College London, London SW7 2AZ, UK
*Corresponding author. E-mail: l.jenkins.1@research.gla.ac.uk

Abstract–Winchcombe is a CM chondrite that fell in England on February 28, 2021. Its rapid retrieval was well characterized. Within two polished sections of Winchcombe, terrestrial phases were observed. Calcite and calcium sulfates were found in a sample recovered from a field on March 6, 2021, and halite was observed on a sample months after its recovery from a driveway on March 2, 2021. These terrestrial phases were characterized by scanning electron microscopy, Raman spectroscopy, and transmission electron microscopy. Calcite veins crosscut the fusion crust and therefore postdate it. The calcite likely precipitated in the damp environment (sheep field) where the meteorite lay for six days prior to its retrieval. The sulfates occur on the edges of the sample and were identified as three minerals: gypsum, bassanite, and anhydrite. Given that the sulfates occur only on the sample's edges, including on top of the fusion crust, they formed after Winchcombe fell. Sulfate precipitation is attributed to the damp fall environment, likely resulted from sulfide-derived H_2S reacting with calcite within the meteorite. Halite occurs as euhedral crystals only on the surface of a polished section and exclusively in areas relatively enriched in sodium. It was likely produced by the interaction of the polished rock slice with the humid laboratory air over a period of months. The sulfates, fusion crust calcite, and halite all post-date Winchcombe's entry into the Earth's atmosphere and showcase how rapidly meteorite falls can be terrestrially altered.

INTRODUCTION

Meteorite falls are typically treated as near pristine with minimal terrestrial alteration, save for the fusion crust. However, there are various processes that they experience after landing that can alter their mineralogical, chemical, and isotopic compositions (Bland et al., 2006; Lee et al., 2021). Unless these processes are considered when studying falls, terrestrial phases can be misidentified as extraterrestrial, leading to incorrect interpretations of the history of their parent body(ies). Knowing what changes meteorite samples have undergone due to terrestrial alteration will allow the mineralogy of meteorites to be better compared to asteroid samples.

Additionally, understanding terrestrial alteration can lead to improved curatorial practices. It is also important to note that sample return missions are key in investigating other planetary bodies as they are the most pristine samples that can be obtained; any terrestrial contamination they will have undergone will be restricted to curatorial practices and sample analysis. Samples returned by the Japan Aerospace Exploration Agency's (JAXA) Hayabusa and Hayabusa2 missions to Itokawa and Ryugu, respectively, and the National Aeronautics and Space Agency's (NASA) OSIRIS-REx missions to Bennu, will be some of the few samples from another planetary body that have not been terrestrially compromised (Ito et al., 2022; Lauretta

et al., 2017; Lee et al., 2021; Nagao et al., 2011; Watanabe et al., 2017).

All meteorites experience terrestrial alteration to some degree, starting from the moment a meteoroid enters the Earth's oxidizing and hydrolyzing atmosphere. During a meteor's initial descent, its exterior surface will experience temperatures of up to 12,000 K over a time period of no more than 40 s (Hezel et al., 2015). Much of its original mass is lost and the meteorite that reaches the Earth's surface is only a fraction of the original meteoroid (Hezel et al., 2015). A distinctive fusion crust will form on the meteorite's outer surface and is host to a variety of high-temperature phases. They can include amorphous phases, anhydrous minerals with textures associated with quenching, and the remnants of phases not destroyed by the rapid temperature increase (Genge & Grady, 1999).

After making it through the Earth's atmosphere, the surviving meteorite may land in any environment, such as a frozen lake (Grossman, 2000), a desert, or even in someone's home (Gattacceca et al., 2021). In the time between a meteorite's fall and when it is recovered, it will be exposed to the terrestrial environment and may undergo a number of changes. The extent to which a meteorite is modified depends on its composition, the environment within which it has landed, and the time it has spent on the Earth's surface before being recovered. Meteorite falls are typically recovered quickly. Finds are often subaerially exposed for thousands of years (Jull et al., 1993), up to 2 Myr in some cases (Drouard et al., 2019), before they are collected; they will experience terrestrial alteration. The effects of terrestrial alteration may include the production of oxides, sulfates, carbonates, sulfides, arsenides, phosphates, hydrous silicates, and/or hydroxides (Bland et al., 2006; Ivanov et al., 2019; Jenniskens et al., 2012; King et al., 2020; Lee et al., 2021; Tyra et al., 2007; Zurfluh et al., 2013); the dissolution of extraterrestrial minerals (Bland et al., 2006; Jenniskens et al., 2012; Lee et al., 2021); and contamination by terrestrial organics and atmospheric hydrocarbons (Cronin & Pizzarello, 1990).

Terrestrial alteration is often treated as if it stops after the meteorite is recovered. This, however, is not the case. Simply being present in the Earth's oxidizing and water-rich atmosphere can be enough to cause metals to alter and terrestrial water to be incorporated into the meteorite (Bland et al., 2006; Lee et al., 2021). For example, pieces of the fall Ivuna (CI1) were stored in different conditions after being received by the Natural History Museum (NHM) in 2008; some fragments were stored in a controlled inert N_2 atmosphere while others were wrapped in fluoropolymer film and kept in an uncontrolled atmosphere. Terrestrial sulfates formed within the fragments that were in an uncontrolled atmosphere within a few years whereas the fragments kept in a controlled atmosphere did not have these terrestrial phases (King et al., 2020). Gypsum is sometimes found in carbonaceous chondrites and although it can be attributed to parent body processes, it is also a common terrestrial weathering product, making interpreting its formation difficult (Losiak & Velbel, 2011).

The growth of terrestrial phases in meteorite falls is not restricted to Ivuna. Orgueil (CI1) is well known to have large veins of terrestrial sulfates, some of which are associated with grains of magnetite, which can also be found throughout the meteorite (Gounelle & Zolensky, 2001, 2014). The magnetite originates from the alteration of pyrrhotite, believed to have occurred on Orgueil's parent body (Gounelle & Zolensky, 2014). Terrestrial sulfates have also been reported in Tonk (CI1), Alais (CI1), and Revelstoke (CI1) (Gounelle & Zolensky, 2001, 2014). Additionally, terrestrial carbonates are reported in Vigarano (CV3) (Abreu & Brearley, 2005), and Fe-Ni metal has been observed altering to oxides in New Concord (L6), Murchison (CM2), and Murray (CM2) (Lee & Bland, 2004; Rubin et al., 2007).

Several procedures undertaken during sample storage, preparation, and data collection can also alter a meteorite. As exemplified by the Ivuna samples, meteorites can be contaminated by both the sample preparation processes (e.g., epoxy, coating) and data collection (e.g., electron beam damage) (King et al., 2020). The use of water during sample preparation may also cause evaporite minerals to grow and/or dissolve (Floyd & Lee, 2021).

The Winchcombe meteorite is a Mighei-like (CM) carbonaceous chondrite that fell in Gloucestershire, United Kingdom, on the evening of February 28, 2021. Although some fragments were recovered on March 1, 2021, within 12 h of the fall, others took weeks to find, with the last documented fragment being collected on April 1, 2021 (Russell et al., 2022). Most of the Winchcombe samples were recovered within the first week of its fall. After retrieval, samples were placed into sealed plastic bags. Despite this rapid collection, Genge et al. (2023) observed electron beam-sensitive calcium oxalates growing within the fusion crust of some samples from the piece of Winchcombe recovered after it spent six days in a sheep paddock after the fall. Additionally, on the same stone, Russell et al. (2022) also observed a white–yellow substance growing on its exterior.

As the fall, recovery, and curation of Winchcombe are very well documented (King et al., 2022; Russell et al., 2022), it is an ideal sample with which to study the effects of terrestrial alteration on CM falls. We describe carbonate, sulfate, and halide phases in Winchcombe that may be interpreted as having a parent body or a terrestrial origin. We argue that these phases formed after

Winchcombe's fall during its brief time exposed to the Earth's environment. This work has important implications for understanding how terrestrially compromised even the newest meteorite falls can be, as well as how curation and analysis may affect both meteorites and returned samples, including those from the C-complex asteroids Ryugu and Bennu.

MATERIALS

Winchcombe is a CM chondrite breccia composed of numerous lithologies. These lithologies have different geologic histories on Winchcombe's parent body and are distinct in their degree of aqueous alteration (Suttle et al., 2022). Here, we focus on two polished rock sections (BM.2022,M2-42 P30540 and BM.2022,M9-14 P30552), each from a different fragment of Winchcombe, each recovered from a different location at a different time after the fall. The fragment from which P30540 was made was collected from a domestic garden lawn on the morning of March 2, 2021. The weather remained dry between the time when Winchcombe fell and when the fragments were recovered by the Wilcock family (King et al., 2022). It was placed into a plastic pot from a supermarket that was, prior to recovery, rinsed with warm water and then cleaned with a dishwasher and dishwashing powder. The fragment from which P30552 was made was collected on March 6, 2021, six days after its fall, from a sheep-grazing field using nitrile gloves and was placed into a plastic bag with other pieces that were coated in soil from the site. Prior to recovery, P30552 was exposed to a damp and humid environment, which although it was free from rainfall, often had dew and potentially frost, experiencing temperatures ranging from −3 to 13 °C and humidity ranging from 44% to 95% (Met Office Weather Observations Website, 2022: Observation Site Bishops Cleeve). About two months after recovery, on May 10, 2021, an amorphous white–yellow phase was observed on its fusion crust (Russell et al., 2022). This material was not recorded during recovery.

On March 5, 2021, and March 8, 2021 the containers were received by the NHM, London and opened. With tweezers and nitrile gloves, the pieces of meteorite were transferred into glass vials with polyethylene caps, which were in turn stored in labeled polyethylene bags and kept within a desiccator until pieces were selected for the preparation of polished sections. The two polished rock sections used in this study (P30540 and P30552) were prepared at the NHM during the first week of May 2021. They were set in epoxy resin and then polished with ethanediol and alumina. The samples were transferred to the University of Glasgow (UoG), where they were kept in plastic boxes in a laboratory environment under ambient conditions.

METHODS

Sample Preparation

An overview of the general sample processing of each sample prior to analysis is shown in Fig. 1. Before data collection using scanning electron microscopy (SEM) and transmission electron microscopy (TEM), the polished sections were coated with 20 nm of carbon. The carbon coat was removed and reapplied every few months. Removal used 0.3 μm alumina glycol or 0.3 μm alumina paraffin on 0.3 μm alumina disks, before being cleaned with ethanol or acetone and patted dry with a Kimwipe. In the Results section, it is stated whether data sets have been collected before or after any reapplication of the carbon coat.

P30540 was also prepared for electron backscatter diffraction (EBSD) analysis as part of a parallel study. For this, the carbon coats were removed using 0.3 μm alumina glycol on 0.3 μm alumina disks, before P30540 was rinsed with distilled water and patted dry with a Kimwipe. P30540 was then polished for 30 min using a vibromat with a 0.1 μm diamond polishing plate, 100 nm colloidal silica in an NaOH (aq) solution. After being polished with colloidal silica, P30540 was wiped with dish soap to remove the colloidal silica and spent 60 s in distilled water in an ultrasonic bath, before being patted dry with a Kimwipe. P30540 was then coated with 7 nm of carbon. The data from P30540 described here were collected prior to preparation for EBSD.

Raman data were collected for P30552 after it had been carbon coated for SEM analysis. To obtain the Raman data, the carbon coat was removed. P30552 was also polished prior to focused ion beam (FIB) work by applying 1 μm diamond suspended in an oil composed of petroleum distillates, quaternium-18 bentonite, and trace amounts of quartz (Buehler MetaDi oil-based monocrystalline diamond suspension) on a 1 μm diamond mat. The sample was cleaned afterward using ethanol and Kimwipes. This polishing took place on May 9, 2022. Note that other electron transparent lamellae were also extracted using the FIB from select areas in both samples prior to collection of any of the data described here. These particular FIB lamellae were not investigated as part of this work, but their extraction process will be discussed where relevant, and results from TEM and atom probe tomography analysis of these lamellae are presented in Daly et al. (submitted).

Microanalysis

Backscattered electron (BSE) and secondary electron (SE) images, and EDS maps and spectra were acquired using a Carl Zeiss Sigma Variable Pressure field emission
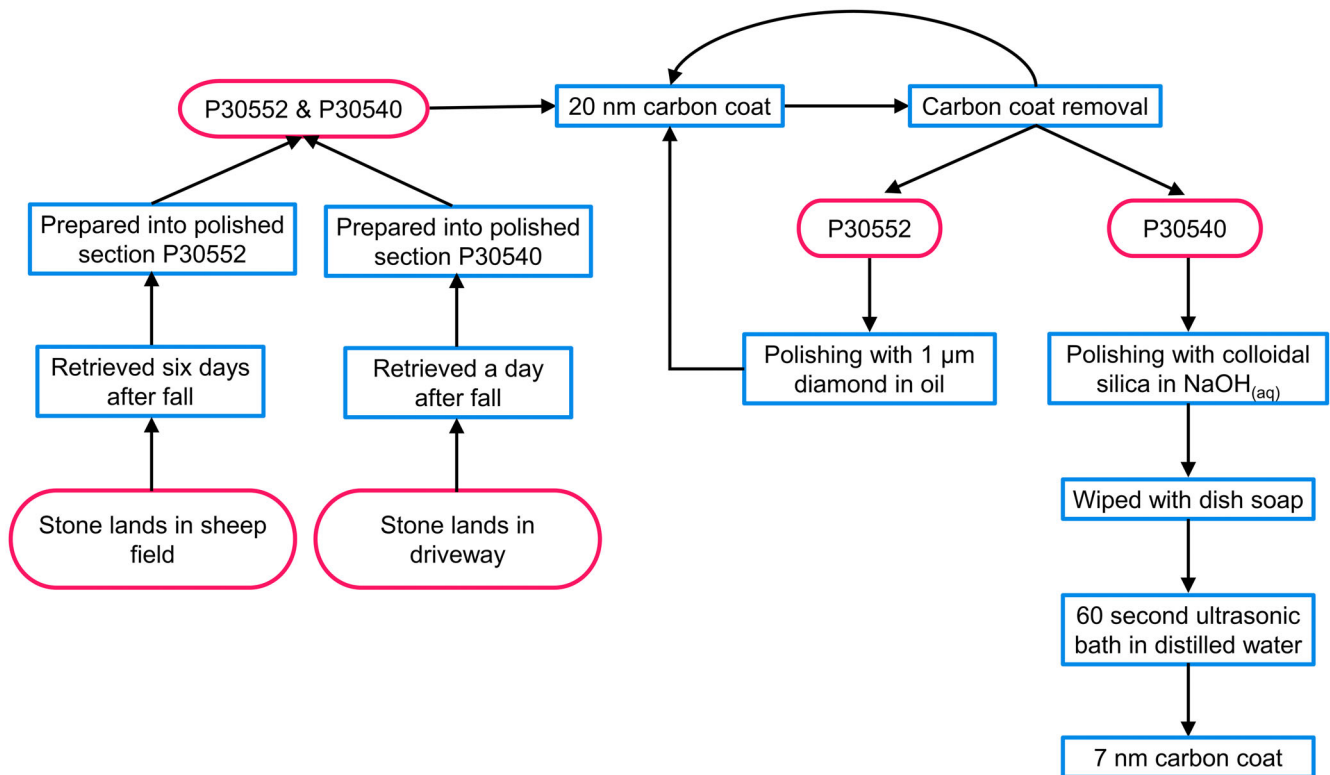
Fig. 1. Overview of the processing polished sections P30552 and P30540 experienced prior to data collection.

gun SEM operated at 20 kV and 1–2 nA at the Geoanalytical Electron Microscopy (GEM) lab, UoG. For the EDS maps and spectra, X-rays were collected using an 80 mm^2 silicon drift detector. BSE images and EDS maps were montaged and analyzed using version 5.1 of the Oxford Instruments AZtec program. Sample P30552 was also studied by cathodoluminescence (CL) using an FEI Quanta 200F Environmental SEM equipped with a KE Developments panchromatic CL detector using the method described by Lee et al. (2014).

Raman data were collected using a Renishaw inVia Raman microscope at GEM using a 514 nm wavelength laser source with a laser power of 45 mW and a spot size of 1 µm. During Raman data collection for P30552, reflected light microscopy was used to navigate around P30552 to find analysis areas. As some of the areas in the carbonates displayed anomalous optical properties, reflected light microscopy was used further to study them.

Electron transparent lamellae were extracted from carbonates in the fusion crust, as well as the sulfates around the edges, of P30552 at the Kelvin Nanocharacterization Centre (KNC), UoG, using a DualBeam FIB microscope. Diffraction-contrast images and selected area electron diffraction (SAED) patterns were collected from the lamellae using an FEI T20 TEM operated at 200 kV in the KNC.

RESULTS

Sample Descriptions

CM chondrites are composed of the primary materials from nebular condensation, including chondrules and calcium-aluminum-rich inclusions (CAIs) along with finer grained materials that form an enclosing matrix as well as rims around chondrules and CAIs. These materials have been aqueously altered to produce a wide range of secondary minerals that may include but are not limited to serpentines (lizardite and cronstedtite), tochilinite, carbonates, and sulfides (Bunch & Chang, 1980). Many CM chondrites are breccias and can be classified in their degree of aqueous alteration based on the relative abundance of primary anhydrous components and their secondary alteration products (Howard et al., 2015). These classifications range CM1–CM3, where CM1 is most altered and CM3 is least altered (Van Schmus & Wood, 1967). For CM2 chondrites, one of the classification systems for degree of alteration further sorts them into subtypes ranging from CM2.0 to CM2.7 (Rubin et al., 2007; Rubin, 2015).

Sample P30540 (Fig. 2) is a polished rock slice in an epoxy puck and is ~6.0 mm^2 in area. It is composed of three clasts, each lithologically distinct: the F lithology,
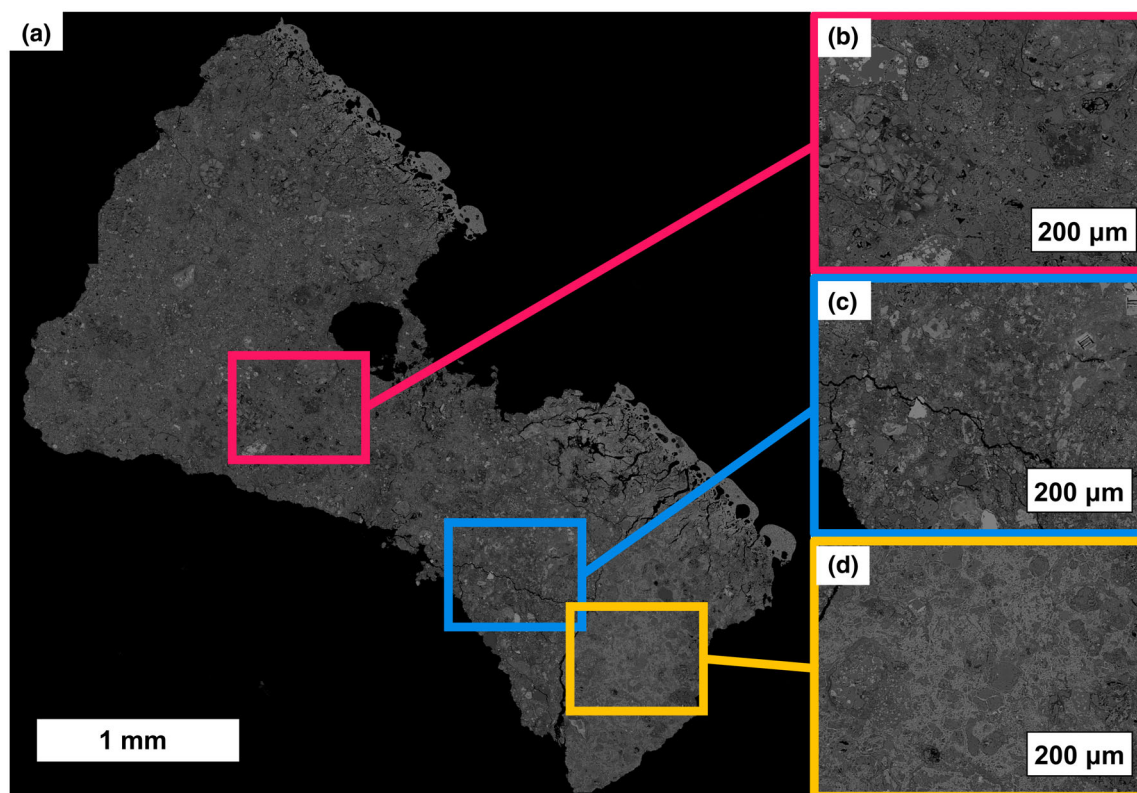
Fig. 2. BSE images of the P30540 polished section of Winchcombe. a) The whole rock sample. b) The F lithology. c) The Mx lithology. d) The G lithology.

the Mx lithology, and the G lithology (Suttle et al., 2022). The F lithology is characterized by its chondrule pseudomorphs and its lack of tochilinite–cronstedtite intergrowths (TCIs), having been extensively aqueously altered. The F lithology is of the petrologic type CM1. The Mx lithology is characterized by its cataclastic nature and is made up of a variety of components, including primary silicate mineral fragments, chondrules, TCIs, fine-grained serpentine-rich matrix, and CAIs. The G lithology is mainly composed of a mixture of fine-grained serpentine-rich matrix and TCIs, with some chondrules (Suttle et al., 2022). As it retains some chondrules, the G lithology is less altered than the F lithology and has a petrologic subtype of CM2.1 The F and G lithologies are in contact with the fusion crust, and all lithologies contain carbonate mineral grains.

Sample P30552 (Fig. 3) is a rock slice ~9.8 mm^2 in area in an epoxy puck. Also within the epoxy puck is 100 μm^2 of soil from the landing site (Fig. 3b). P30552 is composed of two clasts that are both of the A lithology (Fig. 3b and 3d) and are composed of partially altered chondrules among a matrix rich in TCIs and serpentine (Suttle et al., 2022). Lithology A has less altered components than the G lithology and has a petrologic subtype of CM2.2. Lithology A also contains carbonates

(Suttle et al., 2022). Both clasts are in contact with the fusion crust.

Calcite

The fusion crusts of both samples are fractured. Some of the fractures in P30552 are filled by a phase with an elemental composition of C, O, and Ca as determined by qualitative EDS (Fig. 4) and best matches $CaCO_3$. These carbonate veins are about 10–20 μm in width and are uniform in both chemical composition and texture, showing no signs of vesiculation. The carbonate veins are nonluminescent when observed by SEM-CL, thus suggesting that they are Mn-poor (<10 ppm) (Habermann et al., 1996).

Under reflected light, the calcium carbonate has two different appearances. Most of the carbonate is light gray–blue in color, whereas that at the edges of the veins is dark gray (Fig. 5). Although the dark gray appearance of the carbonate at the veins' edges is typical for calcite, the appearance of the light gray–blue phase is not. Raman spectra collected for the dark gray carbonate (Fig. 6a) have peaks at 127, 154, 281, 710, and 1085 cm^{-1}, which best matches calcite (e.g., Kim et al., 2021). Spectra from the light gray–blue phase (Fig. 6b) had very few
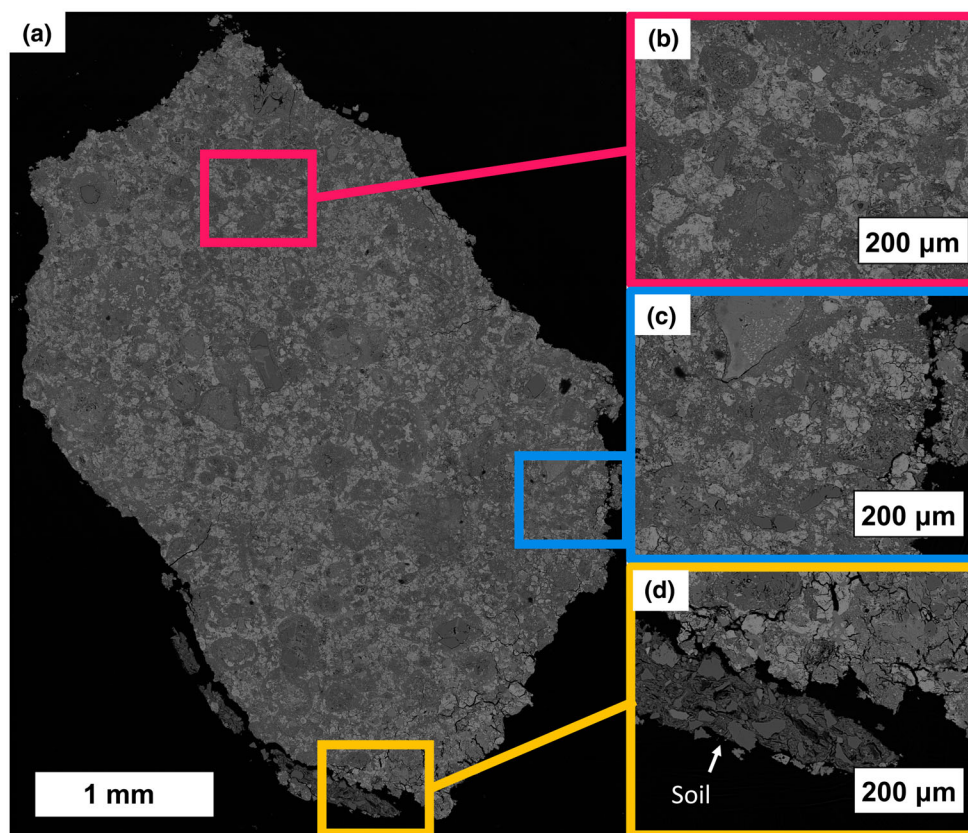
Fig. 3. BSE images of the P30552 polished section of Winchcombe. a) The whole rock sample. b) The larger main clast. c) The smaller clast. d) The soil on the edge of the sample.
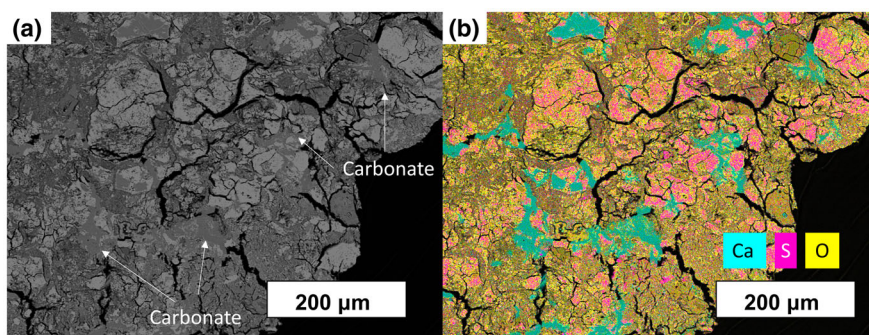

Fig. 4. The fusion crust of P30552 with veins of calcium carbonate. a) BSE image. b) Ca-S-O false color EDS map showing veins of calcium carbonate in turquoise.

peaks, which could be due to the sample being strained, poorly crystalline, or amorphous. Those peaks that were identified are at 284, 1085, and 1261 cm^{-1}, and are again consistent with calcite. Hereafter, the carbonate that has optical properties under reflective light typical for calcite is referred to as "nCal" (normal calcite) and the carbonate that is anomalously reflective is referred to as "RCal" (reflective calcite).

TEM images of the electron transparent lamella produced by FIB for the RCal show a crystalline phase composed of multiple parallel subgrains (Fig. 7). The boundaries between the subgrains display dislocations. Most of the subgrains are in similar crystallographic orientations, save for one subgrain on the very edge, which likely belongs to the nCal. The SAED patterns acquired for all subgrains indexed as calcite.
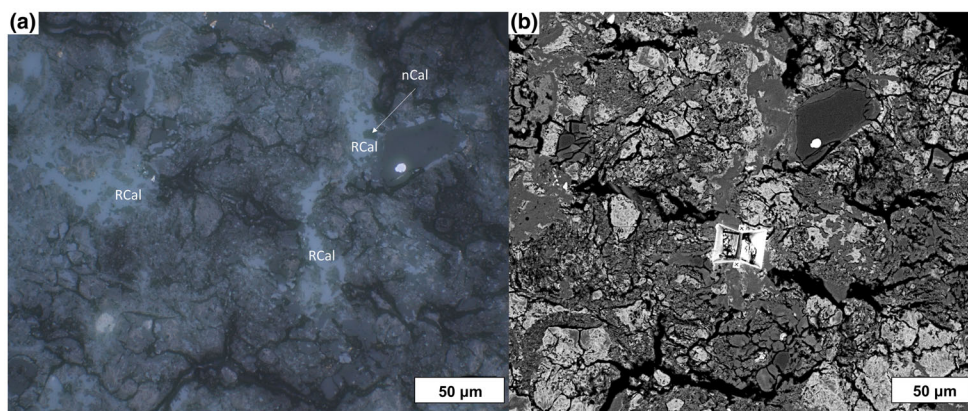
Fig. 5. Images of calcite in P30552. a) Reflected light image. The dark gray phase is nCal, while the light blue–gray phase is RCal. b) BSE image of the same area in (a) taken on May 17, 2022, after an electron transparent lamella was extracted using FIB.
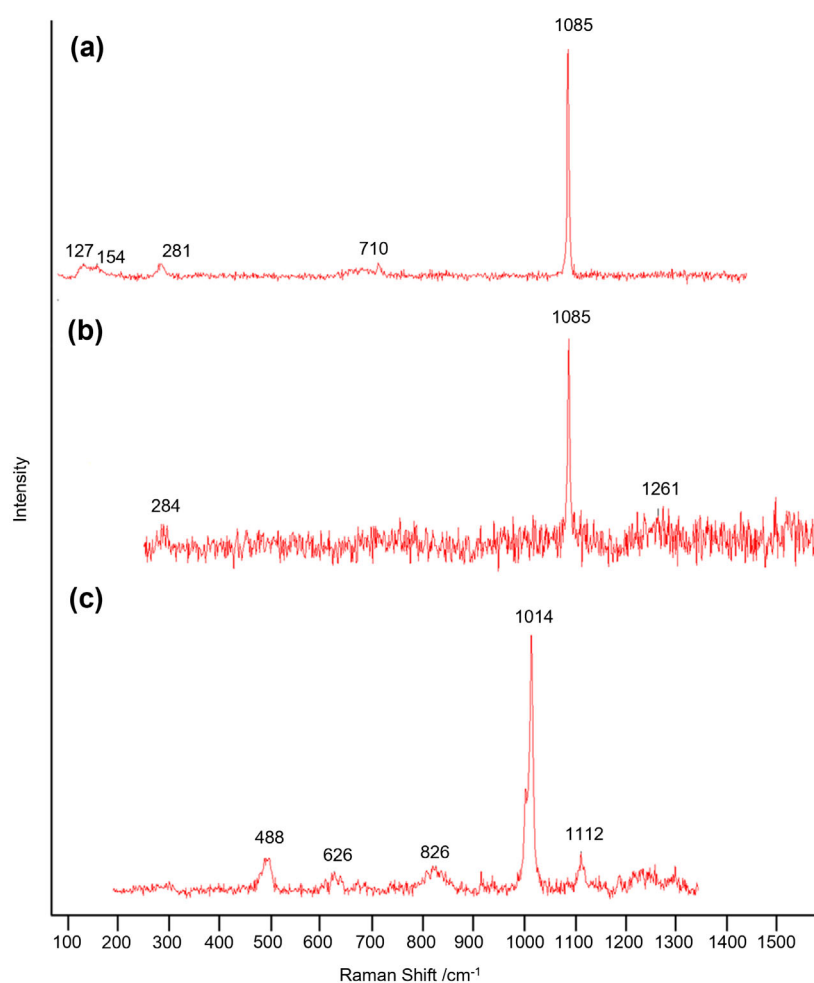

Fig. 6. Raman spectra from P30552. a) For the dark gray phase matching calcite, referred to as nCal. b) For the light gray–blue phase whose few peaks match calcite, referred to as RCal. c) For sulfates which best match bassanite.

Calcium Sulfates

The BSE images, and EDS and Raman data relating to the sulfates in P30552 were collected on different dates (September 14, 2021; November 1, 2021; January 13, 2022) between which the carbon coat had been removed and reapplied. EDS maps show that a Ca, S, and O-rich phase (likely calcium sulfate) occurs exclusively on the
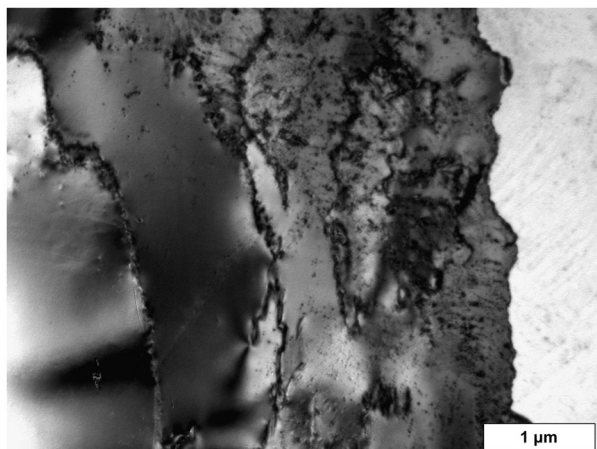
Fig. 7. Bright-field TEM image of an FIB section of carbonates taken from the RCal in P30552. Most of the subgrains (dark gray) are in a similar crystallographic orientation except for the subgrain (white) on the rightmost edge.

edges of the sample in patches that range in size from 10 to 130 μm (Fig. 8a) and is not present anywhere else within the meteorite. One of these areas is on top of the fusion crust (Fig. 8b). There are also small patches of calcium sulfate on the outer edge of the adhering soil, but not within the soil itself. BSE images show that the calcium sulfate is embedded within the epoxy (Fig. 8c), and there are multiple instances of the calcium sulfates being in contact with calcite. The phase must be soft and friable because images of the same areas before and after removal and reapplication of the carbon coat show that it has degraded (Fig. 9a and 9b). Raman spectra of the calcium sulfates have several peaks whose closest match are bassanite, although some peaks match gypsum and/or anhydrite better (Fig. 6c; Table 1). It is thus likely that the calcium sulfate is primarily bassanite intergrown with minor amounts of gypsum and anhydrite. Two of the spectra show peaks centered ~820 cm^{-1} that likely originated from a nearby phase, although there is insufficient data to identify it.

TEM images were collected on June 15, 2022, for an FIB lamella extracted from an area of calcium sulfate. The TEM images show that the FIB section contains a high density of pores, many of them elongate and sinuous, up to ~1 μm in length (Fig. 10a). Within the calcium sulfate are patches of finely crystalline phyllosilicate up to a couple of micrometers in size (Fig. 10a). Individual calcium sulfate crystals are submicrometer in size. SAED patterns acquired with a large 4 μm diameter aperture yielded broken rings. The strongest reflections have d-spacings of 0.600, 0.344, 0.300, and 0.275 nm, which are indicative of bassanite lattice spaces with miller indices (100), (310), (200), and ($\bar{1}$14), respectively (Fig. 10b). These reflections are consistent with previous SAED work on bassanite in

carbonaceous chondrites (Lee, 1993) and synthetic materials (Anduix-Canto et al., 2021). If gypsum or anhydrite were present, reflections would be expected with d-spacings of 0.458 nm for the miller index (021) for gypsum (Saha et al., 2012), and 0.350 nm for the miller index (200) for anhydrite (Lee, 1993). None of the gypsum or anhydrite reflections were observed. Bassanite is the main calcium sulfate present within Winchcombe and is the only sulfate composing the FIB lamella; however, the gypsum and anhydrite observed with Raman likely exist in small quantities within Winchcombe.

Halite

All of the data relating to halite in P30540 were collected on September 11, 2021, prior to any carbon coat removals and prior to the sample being polished for EBSD. EDS maps show that Na is concentrated in small patches in serpentine-rich areas of the Mx and G lithologies (Fig. 11a). The Na-rich area in the Mx lithology has been previously targeted by FIB sample preparation techniques (Fig. 11b). Higher resolution BSE images and EDS maps show that this concentration of Na is related to a phase composed of both Na and Cl (Fig. 11b and 11c). SE images collected for the NaCl phase show that it occurs as euhedral cubes sitting on top of the sample's polished surface (Fig. 11d). Due to both the chemical composition and cubic crystal shape of the NaCl phase, it is identified as halite. Nearby the halite are areas within the fine-grained matrix that are enriched in Na, but not Cl.

DISCUSSION

There are three potentially terrestrial alteration phases observed within Winchcombe samples P30540 and P30552: calcite, calcium sulfates (bassanite, gypsum, and anhydrite), and halite. Due to the petrographic contexts of these three alteration phases occur in, we argue that they are terrestrial in origin. In some other CM chondrite falls (e.g., Murchison, Cold Bokkeveld), sulfates and halite have been observed in similar contexts; however, they are usually attributed to parent body processes (Barber, 1981; Lee, 1993; Lee et al., 2021). Regarding sulfates, when a terrestrial origin is posited for them in CM chondrites, the time scale given for their growth is reported to be a few years (Fuchs et al., 1973; Lee et al., 2021).

Calcite

Some of the calcite in P30552 infills fractures in the fusion crust that formed as the meteoroid entered the
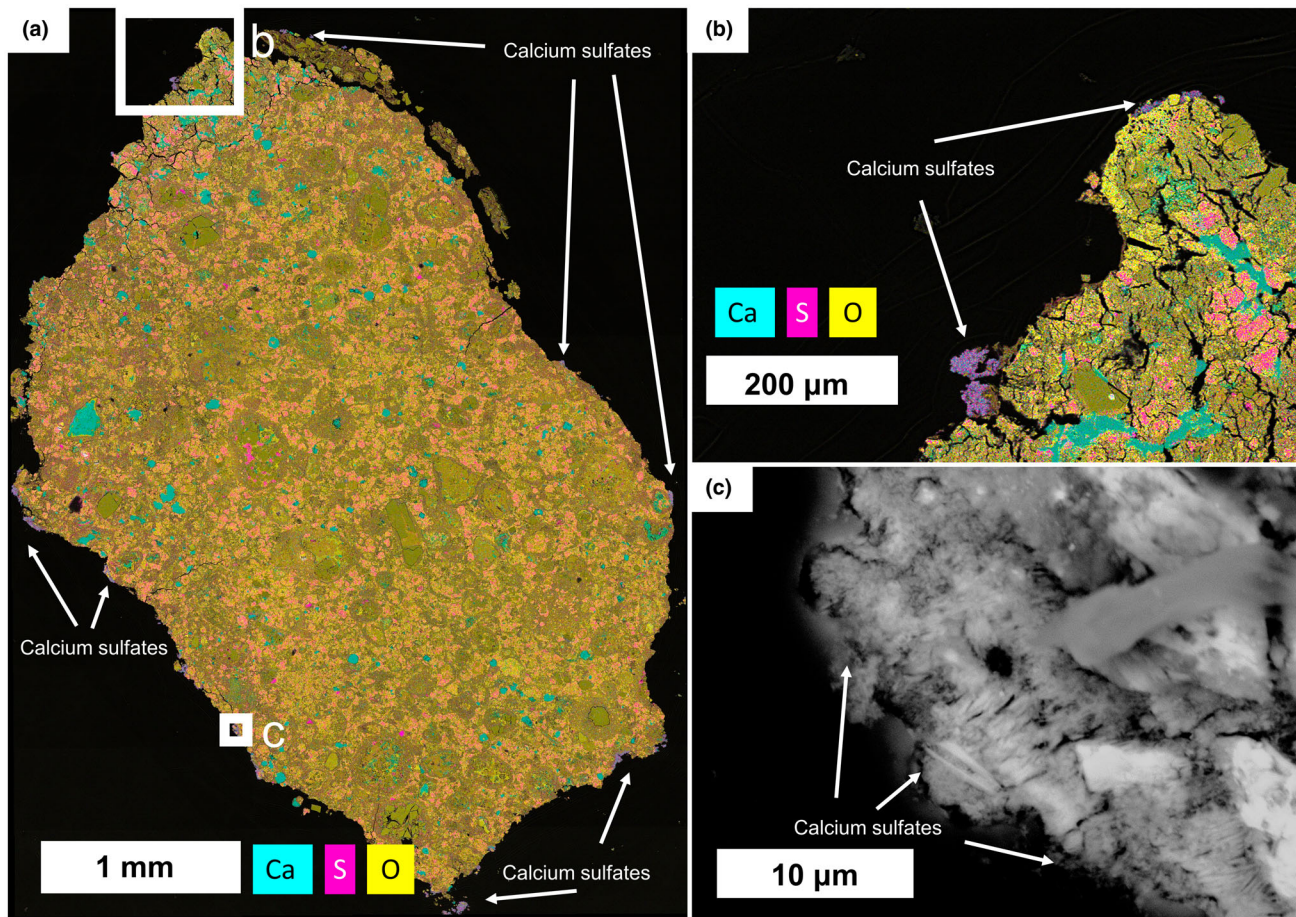
Fig. 8. Calcium sulfates in P30552. a) Ca-S-O EDS map of whole sample. Calcium sulfate can be seen along the sample's edges in purple. b) Ca-S-O EDS map of the fusion crust. Clumps of calcium sulfate occur on the exterior of the fusion crust. c) BSE image of calcium sulfate showing it embedded within the epoxy.

Earth's atmosphere. If the calcite deposition was synchronous with fracture formation, then it is likely to have originated as a high-temperature carbonate melt. If its deposition occurred after fracturing, then the calcite is a terrestrial alteration phase that precipitated after the meteorite's landing.

Carbonate melts occur on Earth at pressures exceeding 4 MPa or when fluorine is incorporated into the melt (Gozzi et al., 2014). When a meteor enters the Earth's atmosphere, it experiences temperatures in the range of 2000–12,000 K and 2–5 MPa of pressure (Hezel et al., 2015). Thus, it is possible for carbonate melts to form under these conditions; however, analog experiments on fusion crust formation have yet to produce carbonate melts; carbonates usually decompose into CO_2 gas and oxides instead (Brandstätter et al., 2008). It is also important to note that the calcite veins in Winchcombe do not show any quench textures or vesiculation (Fig. 5) that would support formation as a carbonate melt. Finally, modeling of the peak pressures experienced by the Winchcombe meteoroid during atmospheric entry show that it reached only 0.6 MPa (King et al., 2022; McMullan et al., 2023), and therefore, a carbonate melt would not have been stable during Winchcombe's atmospheric entry and is unlikely to have formed the calcite veins.

It is therefore most probable that these calcite veins formed after the fusion crust, likely from a precipitate, either during the six days that the stone P30552 was made from spent in a field, or during the two months prior to the polished section P30552 being prepared. Terrestrial carbonates typically form in meteorites when atmospheric CO_2 reacts with Ca and other ions dissolved in liquid water in contact with the meteorite (Bland et al., 2006). Precipitation of P30552 calcite veins under low-temperature and oxidizing conditions is consistent with its non-luminescence, which reflects low concentrations of Mn (<10 ppm) and is typical of carbonates that have formed at the Earth's surface in other contexts, such as speleothems (Richter et al., 2018).
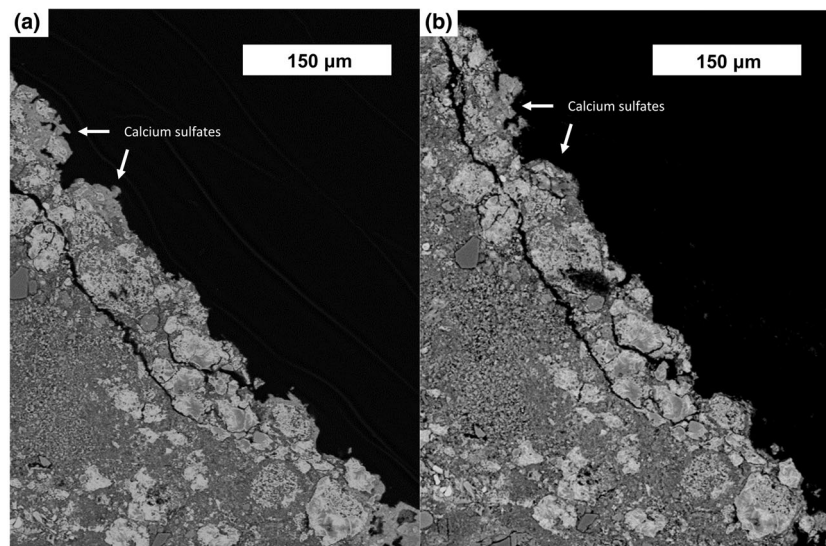
Fig. 9. Degradation of calcium sulfates in P30552. a) BSE image of an area with calcium sulfates taken on September 14, 2021. Calcium sulfates, among other phases, can be seen on the meteorite's edge. b) BSE image of the same area as (a) taken on November 1, 2021. Although some of the calcium sulfates remain, others are missing.

Table 1. Raman peak positions for gypsum, bassanite, anhydrite (from Liu et al., 2009), and for the spectra collected from the calcium sulfate phase.

Gypsum	Bassanite	Anhydrite	Spectra 1	Spectra 2	Spectra 3
415		416			
	427				
439					
	489	499	492	484	493
		612			
620	628	629	626	625	638
670	668	676			
				820	826
1008				1002	
	1015	1017	1014	1014	1014
		1110	1111	1113	1112
1135	1128	1128			
		1159			

The scenario of calcite veins within the fusion crust being the result of terrestrial weathering post-fall is thus plausible and is supported by the presence of Ca-oxalate that formed by post-fall terrestrial alteration of another sample of Winchcombe that was also made from the same stone (Genge et al., 2023).

There are two distinct phases of calcite defined by their optical properties in reflective light. There is nCal, which has typical optical properties for calcite, and RCal, which has an anomalously high reflectivity. The RCal constitutes the majority of the fusion crust's carbonate, while the nCal is restricted to isolated patches and the veins' edges (Fig. 5). The differences in reflectivity between RCal and nCal are unusual as they are chemically identical and the RCal's Raman spectra do not match any other known polymorph of calcium carbonate. One possibility is that the differences in optical properties are due to crystallographic orientation. Minerals that display bireflectance, like calcite, will reflect light differently depending on their orientation (Ebert et al., 2009). However, there are very few studies on non-ore minerals under reflected light at visible light wavelengths, and as a result, there is little documentation on how calcite's optical properties vary in reflected light microscopy. All the grains of the RCal typically grow in a similar crystallographic orientation (Fig. 7), and it is possible that the rapid crystallization of the calcite allowed it to preferentially grow in a set of similar orientations. It is likely that the high reflectance of the calcite is due to this orientation and P30552 happened to be cut in a way that made it highly reflective. The rapid growth may have also led to the RCal being strained, resulting in a Raman spectrum with few peaks. The nCal typically occurs on the vein's edges, in contact with other phases like phyllosilicates and TCIs. It is likely that edges of the fractures offered a solid surface for the nCal to nucleate on at a different orientation to the rest of the RCal, forming the thin layer of nCal observed.

Winchcombe is also not the first meteorite fall with terrestrial carbonates. Vigarano (CV3) is also reported to have veins of carbonate. The carbonate veins in Vigarano are the result of terrestrial alteration of a piece of the meteorite that spent a month outdoors during the winter in the Ferrara province of Italy after it landed on January 22, 1910 (Abreu & Brearley, 2005). The carbonates within Vigarano are more abundant than they are in
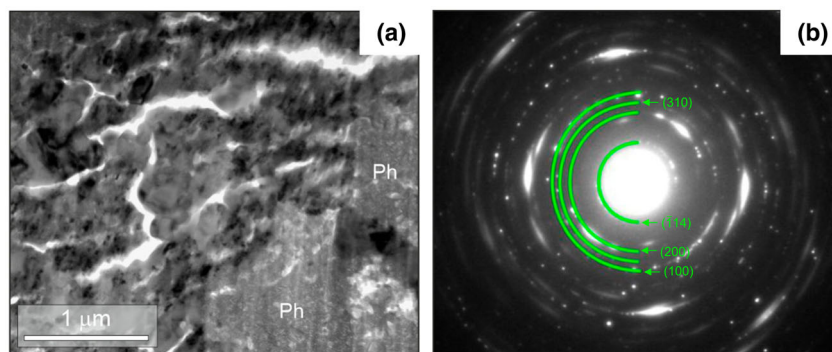
Fig. 10. a) Bright-field TEM image of an area of calcium sulfate, which is finely polycrystalline and contains patches of phyllosilicate (Ph). The sinuous white features are pores. b) SAED pattern of the calcium sulfate. The innermost four rings have been highlighted in green and are attributable to the (100), (310), (200), and ($\bar{1}$14) miller indices of bassanite.
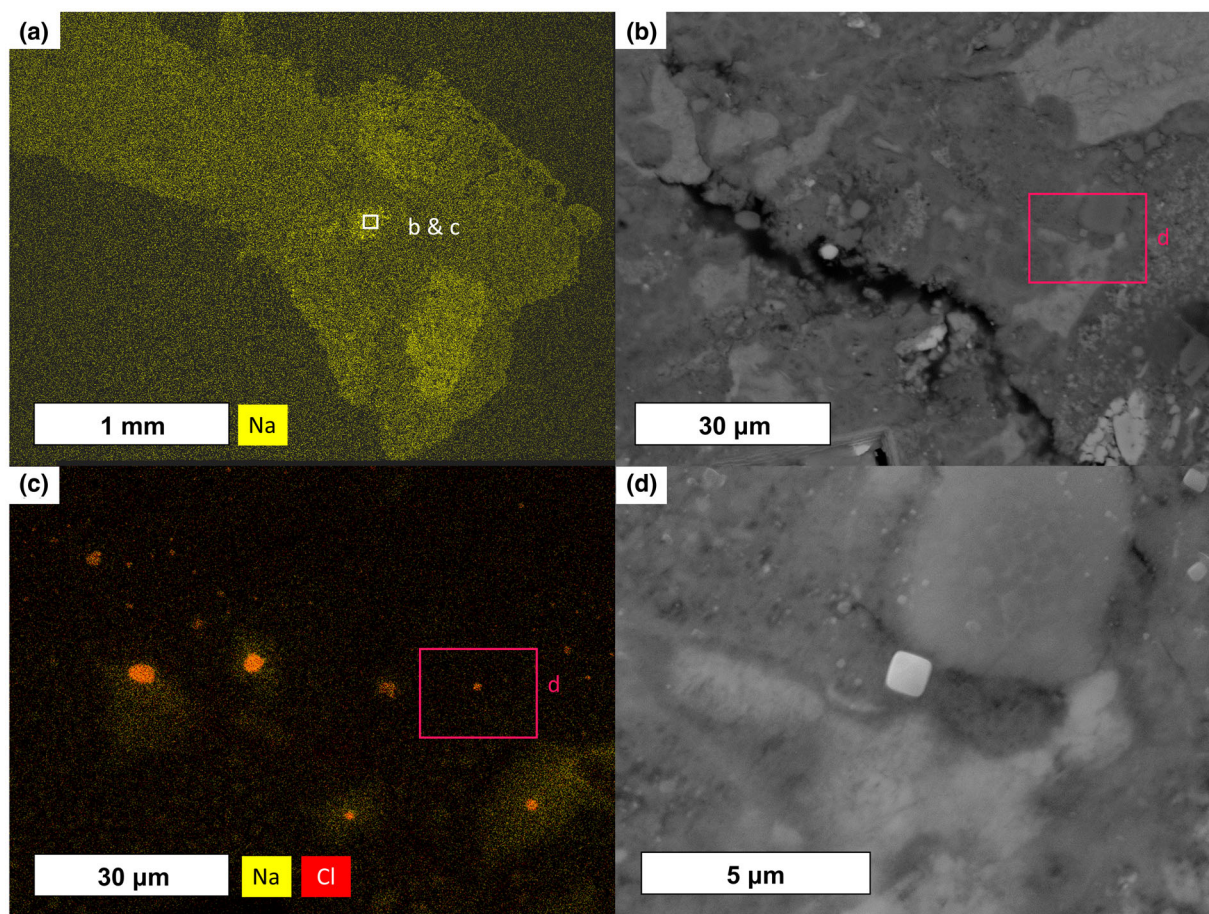

Fig. 11. Na-rich areas in P30540. a) Na EDS map of Mx and G lithologies. The white box indicates the area depicted in (a) and (b). b) BSE image of an Na-rich area within the Mx lithology. The edge of an FIB pit can be seen on the bottom left-hand side of the image. The pink box indicates the area depicted in (d). c) Na and Cl EDS map of an Na-rich area within the Mx lithology showing NaCl in orange. The pink box indicates the area depicted in (d). d) SE image of NaCl phase in the Na-rich area. The NaCl cube in the center of the image is bright indicating that it is sitting on top of the sample's surface.

Winchcombe because Vigarano spent a longer time subaerially exposed. Thus, there is a historical precedent for the calcite veins within the fusion crust of Winchcombe to be products of terrestrial alteration.

Calcium Sulfates

Calcium sulfates are common terrestrial alteration products for carbonaceous chondrites that are Antarctic
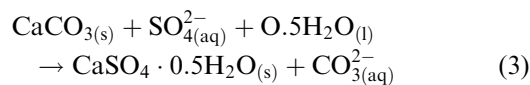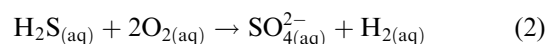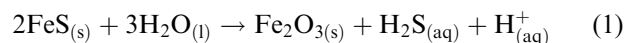
finds (Losiak & Velbel, 2011). However, these minerals have also been reported in carbonaceous chondrite falls, including Cold Bokkeveld, Orgueil, and Ivuna (Gounelle & Zolensky, 2001; King et al., 2020; Lee, 1993). Regarding Ivuna, euhedral crystals of gypsum have been previously observed on top of the polished section, consistent with a terrestrial origin (King et al., 2020). However, Cold Bokkeveld contains calcium sulfates occurring in several generations and habits, indicating multiple precipitation events under varying conditions, such as what would be expected to occur during parent body aqueous alteration (Lee, 1993).

Calcium sulfates in Winchcombe P30552 are embedded in epoxy, and therefore, they must have grown before the sample was prepared on May 3, 2021. A terrestrial origin for these sulfates requires rapid growth occurring over a period no longer than two months. However, there is petrographic evidence for its post-fall formation. The sulfates occur only on the outer edges of P30552, which are also likely the outer edges of the meteorite, and on top of the fusion crust. Bassanite, the main sulfate observed, breaks down into anhydrite (CaSO$_4$) at about 390 K (Ballirano & Melis, 2009) and anhydrite decomposes into CaO and SO$_3$ gas at about 1670 K (Newman, 1941); neither mineral could have survived the high temperatures of fusion crust formation. Furthermore, if the sulfates formed on Winchcombe's parent body, they should be found throughout the meteorite, not just on its edges. Therefore, the calcium sulfates in P30552 are terrestrial in origin and show that these minerals can form rapidly within months of the fall.

Ivuna-like carbonaceous (CI) chondrites also commonly have terrestrial sulfates that are reported to form over time scales on the order of years (Gounelle & Zolensky, 2001; King et al., 2020). CI chondrites also contain sulfates that are reported to be extraterrestrial due to being observed only weeks after their retrieval (Gounelle & Zolensky, 2001). However, these sulfates might be terrestrial as well; sulfate growth within Ivuna has been induced in a laboratory setting using ethanol over a time period of only 3 days (Gounelle & Zolensky, 2001), and CI-like samples returned from the asteroid Ryugu by Hayabusa2 are devoid of sulfates (Yokoyama et al., 2022). Given that the sulfates within Winchcombe formed quickly, the growth of terrestrial sulfates in CI chondrites could have been just as rapid.

The sulfates are likely to have formed as a by-product of the alteration of various minerals within Winchcombe. Like other CM chondrites, Winchcombe contains abundant sulfides (e.g., pentlandite, pyrrhotite) and carbonates (e.g., calcite and dolomite) (Suttle et al., 2022). Bassanite is metastable and can be formed by the dehydration of gypsum at temperatures of at least 368 K (Strydom et al., 1995), by the rapid quenching of calcium

sulfate solutions, or as a precursor phase to gypsum (Tritschler et al., 2015). Terrestrially, sulfates can form during the evaporation of brines (Hardie & Eugster, 1970) or from a series of reactions, whereby sulfides (e.g., pyrrhotite) dissolve in water to form H$_2$S that is then oxidized to SO$_4^{2-}$, which in turn reacts with calcium carbonate in a hydrous environment to form calcium sulfates (Galdenzi & Maruoka, 2003; Hose & Rosales-Lagarde, 2017; Pirlet et al., 2010). This reaction is exemplified by Equations 1–3, derived from Pirlet et al. (2010), which assume that pyrrhotite is the sulfide being altered and that the oxidization product is magnetite; oxidation of pyrrhotite to magnetite can result from the alteration of carbonaceous chondrites by water (Trigo-Rodríguez et al., 2019). Both gypsum and bassanite can also be produced synthetically, for example, by flue gas desulfurization in coal power plants, where SO$_x$ gas reacts with Ca-bearing minerals, like calcite and portlandite, to produce calcium sulfates (Ambedkar et al., 2011; Caillahua & Moura, 2018; Hajar et al., 2016).

$$2FeS_{(s)} + 3H_2O_{(l)} \rightarrow Fe_2O_{3(s)} + H_2S_{(aq)} + H^+_{(aq)} \quad (1)$$

$$H_2S_{(aq)} + 2O_{2(aq)} \rightarrow SO^{2-}_{4(aq)} + H_{2(aq)} \quad (2)$$

$$CaCO_{3(s)} + SO^{2-}_{4(aq)} + O.5H_2O_{(l)}$$
$$\rightarrow CaSO_4 \cdot 0.5H_2O_{(s)} + CO^{2-}_{3(aq)} \quad (3)$$

SAED patterns and TEM bright-field images only identify bassanite (Fig. 10); however, Raman spectra shows peaks that can be attributed to gypsum and anhydrite in addition to the bassanite peaks (Table 1). It is likely all three sulfates are present with bassanite being the most abundant. It is possible that bassanite and anhydrite formed alongside gypsum, as its precursor phases, or as dehydration products. Given the damp, humid, and cool conditions of the Winchcombe sheep field, gypsum dehydration is unlikely to be the source of bassanite and anhydrite. P30552 spent six days in a damp and oxidizing environment, and the calcium sulfates on the edges of P30552 are often in contact with calcite, making the reaction between dissolved sulfides and carbonates within the meteorite the most likely scenario for the sulfates' formation. This mechanism is also the likely source of sulfates in other falls, such as CI chondrites.

Halite

Halite occurs as euhedral cubes that sit on top of the polished rock slice of P30540 (Fig. 11d). This mode of occurrence indicates that the halite formed after the sample had been prepared into a rock slice and embedded

into an epoxy puck. The P30540 sample had not been exposed to any fluids at the time of SEM data acquisition. The halite therefore formed in the months between the polished sample being produced on May 3, 2021, and the SEM imaging on September 11, 2021. It occurs only in specific areas within the P30540 sample and is not pervasive throughout the meteorite.

This is not the first report of halides within a CM chondrite. Barber (1981) has reported halite and sylvite in Murchison (CM2). These crystals were euhedral, similar in morphology to the halite in Winchcombe. The halides Barber (1981) observed were found on a relatively recently prepared thin section that had not been in any contact with water. As a result, Barber (1981) interpreted them to be pre-terrestrial. However, as the terrestrial halite-bearing section of Winchcombe P30540 had also not been in any contact with liquid water, it is possible that the halides observed by Barber (1981) were also terrestrial.

The order in which evaporite minerals crystallize is dependent on the proportions of ions within a system, with halite crystallizing when there is a significant proportion of Na^+ and Cl^- (Hardie & Eugster, 1970). Carbonaceous chondrites typically do not have a significant source of Na^+ for halite and tend to precipitate Mg-rich phases when terrestrially weathered (Izawa et al., 2010), which makes the occurrence of halite in Winchcombe unexpected. Additionally, given the relatively high S abundance in carbonaceous chondrites, sulfates are more likely to precipitate than halides (Fanale et al., 2001; Hardie & Eugster, 1970; Izawa et al., 2010). Carbonaceous chondrites that have areas with significant amounts of Na^+ may have contributions from cometary material (Nittler et al., 2019); however, no evidence of cometary material has been identified in Winchcombe so far.

Regarding the source of Na for the halite within the meteorite, Na-rich minerals that may occur in carbonaceous chondrites are montmorillonite, panetheite, blödite, saponite, Na-phlogopite, nepheline, sodalite, melilite, and plagioclase (Barber, 1981; Brearley, 2006; Lee et al., 2019; Nakamuta et al., 2006; Rubin, 1997; Schrader et al., 2015). Carbonates in CM chondrites tend to have higher amounts of Na than is usual for terrestrial calcites (Riciputi et al., 1994). Additionally, there are a number of Na-bearing phosphate minerals known to occur in iron meteorites (Rubin, 1997). One of these Na-bearing phosphate minerals, buchwaldite, was observed within the P30540 section of Winchcombe, although it occurs in the F lithology and not where the halite was observed. Any one of the minerals listed could be a potential source of Na to facilitate the precipitation of terrestrial halite in carbonaceous chondrites. Daly et al. (submitted) also found Na concentrated in the

boundaries between cronstedtite and lizardite in TCIs in section P30552 using FIB-based time of flight secondary ion mass spectrometry and atom probe tomography. This serpentine boundary concentrated Na may also be a source of Na for the halite, especially as the mobility of elements is elevated along grain boundaries (Lee, 1995; Reddy et al., 2020) and water may trap positive ions like Na on the edges of minerals (Trigo-Rodríguez et al., 2019).

Within Winchcombe itself, the non-halite Na does not appear to be associated with P, ruling out any Na-phosphates as the source of Na. There is also not a significant amount of Al or Ca associated with the Na, discounting any aluminosilicates and Ca-bearing minerals as Na sources. This leaves the following three possibilities for the Na source: an Na-bearing phyllosilicate like Na-montmorillonite, an Na-sulfate like blödite, or Na concentrated in the boundaries between minerals. The latter is the most likely source as it has been observed by Daly et al. (submitted) in TCIs that have replaced carbonates within P30552; however, none of the possible sources for the Na have been positively identified in the fine-grained matrix. Future studies with atom probe tomography may be able to confirm the source of Na.

Comparison to Other CM Falls

At the time of writing, the Winchcombe meteorite is one of 21 known CM chondrite falls. A year before Winchcombe fell, on August 1, 2020, Kolang (CM1/2) landed in Kolang, Indonesia. The main mass fell in a coffin-maker's home, while the rest of the meteorite fell in a rice paddy. The majority of the meteorite was recovered within seconds to hours of it falling (Gattacceca et al., 2021). Kolang is a CM1/2 chondrite that is, like Winchcombe, a rapidly recovered breccia. However, to date, there are no reports of sulfates or fusion crust carbonates within Kolang. It is important to note that the method of retrieval for Kolang (e.g., with or without gloves), was not recorded.

Three years before Kolang, on November 27, 2017, Shidian (CM2) fell in the Yunan Province of China, landing in the areas around two villages (Fan et al., 2020). Within hours of the fall, many of the pieces were recovered (Shijie Li, personal correspondence). Shidian is similar to Kolang and Winchcombe in its overall degree of aqueous alteration (Fan et al., 2020; King et al., 2021; Suttle et al., 2022); however, its degree of terrestrial alteration is more similar to Kolang than Winchcombe as there are no reports of sulfate growth within Shidian at the time of writing. The retrieval process for Shidian was also not recorded.

In September 1969, the well-known CM2 chondrite, Murchison, fell in Australia. Some fragments were

retrieved hours after the fall (Botta & Bada, 2002), but others were not recovered until months later in February and March of 1970 (Kvenvolden et al., 1970). Although the majority of Murchison exhibits less parent body aqueous alteration than Winchcombe (Rubin et al., 2007; Suttle et al., 2022), it contains similar alteration phases to Winchcombe that may have a terrestrial origin, including halite and sulfates (Barber, 1981; Fuchs et al., 1973). Some sulfates are observed within the meteorite itself, typically associated with calcite (Armstrong et al., 1982) and within the meteorite's fractures (Fuchs et al., 1973). Whether the sulfates in Murchison are terrestrial or extraterrestrial has yet to be conclusively confirmed. If terrestrial, it is assumed that the extended time some of the Murchison samples spent subaerially exposed before retrieval, the environment it was curated in, and/or its overall age led to the proliferation of terrestrial sulfates throughout the meteorite.

Cold Bokkeveld is the oldest CM2 chondrite fall, having landed in South Africa in 1838 (Lee, 1993). The Cold Bokkeveld meteorite fragmented and landed in a variety of environments ranging from fields to swamps; however, many of the fragments were recovered almost immediately after the fall (Maclear, 1840). Cold Bokkeveld is known to have abundant sulfate phases occurring in a variety of morphologies that crosscut each other, indicating multiple generations of alteration. Whether these sulfate generations are terrestrial or extraterrestrial is currently unknown (Lee et al., 2021). The fibrous morphology of some of the calcium sulfate within Cold Bokkeveld indicates that, like Winchcombe, its calcium sulfates grew quickly. Unlike Winchcombe, the sulfates within Cold Bokkeveld are not restricted to the outside edges of the meteorite and occur along fractures and patches within the meteorite itself, in a similar manner to the sulfates observed in Murchison (Lee, 1993).

Older CM falls like Murchison and Cold Bokkeveld typically contain more sulfates than younger CM falls, although whether these sulfates are extraterrestrial or terrestrial is often unknown. In the short term, the amount of terrestrial phases observed is primarily affected by the time exposed to outdoor conditions before retrieval. This can be seen in not only the stark difference in degree of terrestrial alteration between Winchcombe samples but also between Winchcombe and other recent CM falls like Shidian and Kolang. The Winchcombe sample P30540, which was recovered within hours of falling, only shows halite precipitating on the surface of certain areas of the meteorite as a result of it being stored in a non-inert atmosphere and having areas with an unusual enrichment in Na, whereas the Winchcombe sample P30552, recovered from a damp sheep field a week after falling, has terrestrial carbonates in its fusion crust and terrestrial sulfates growing along its edges. Neither Kolang nor Shidian show any immediate signs of terrestrial alteration (beyond the formation of their fusion crusts) despite being older than Winchcombe. It is likely that their near immediate retrieval is the reason for the minimal levels of terrestrial alteration observed so far. All three meteorite falls will probably become more terrestrially altered with time and will likely show signs of oxidation unless they are stored in an inert atmosphere. To understand the terrestrial alteration of carbonaceous chondrites in the long term, it is imperative that these more recent falls are periodically assessed for the presence and abundance of sulfates and other alteration phases. Additionally, by studying how terrestrial alteration may occur in falls, better protocols for sample storage and curation can be developed for both meteorite falls and samples returned by missions (e.g., Herd et al., 2016).

CONCLUSIONS

Winchcombe is a relatively fresh meteorite fall, but within it are a variety of terrestrial phases that formed over different time scales. Carbonates precipitated within the fusion crust in a damp environment, while those same damp conditions produced calcium sulfates, primarily bassanite, from the reaction of calcite with dissolved sulfides. It took no more than two months for both the carbonates and sulfates to form from the six days the sample spent in the damp field. In addition, laboratory storage of P30540 in a non-inert atmosphere allowed halite to precipitate on areas of the meteorite that are enriched in Na. The precipitation of halite took place in two months. The formation of these phases showcases how rapid terrestrial alteration can be.

Terrestrial alteration begins to occur the moment a meteorite enters the Earth's atmosphere, and thus, meteorite falls cannot be completely pristine. Assuming that a meteorite has escaped terrestrial alteration can lead to incorrect interpretations regarding certain phases, like evaporites. The extent of terrestrial alteration developed from the fall site can be limited by rapid recovery and appropriate curation of the sample. Thus, when studying meteorites, it is important to keep in mind how long the sample has spent on the Earth's surface and in what environment, as well as the procedures that were used in sample storage, preparation, and data collection. It is also important to consider the petrographic contexts of various minerals as this is not only good practice for understanding the processes the meteorite has experienced but will yield clues as to whether a given phase is terrestrial or extraterrestrial in origin.

Rapid retrieval of a meteorite can mitigate terrestrial alteration; however, even then alteration (e.g., halite precipitation) may still occur, as the Earth's atmosphere is hydrolyzing and oxidizing. To mitigate this, rapidly

recovered falls need to be stored in an inert atmosphere. The most pristine samples of asteroids that can be acquired are from missions like Hayabusa2 and OSIRIS-REx. This is one of the many reasons why sample return is critical to expanding our knowledge of the solar system. Understanding weathering of meteorite falls will help improve curation protocols for these asteroidal samples and aid in relating them to terrestrially altered meteorites.

Editorial Handling—Dr. Josep M. Trigo-Rodríguez

REFERENCES

Abreu, N. M., and Brearley, A. J. 2005. Carbonates in Vigarano: Terrestrial, Preterrestrial, or Both? *Meteoritics & Planetary Science* 40: 609–25.

Ambedkar, B., Nagarajan, R., and Jayanti, S. 2011. Ultrasonic Coal-Wash for De-Sulfurization. *Ultrasonics Sonochemistry* 3: 718–26.

Anduix-Canto, C., Levenstein, M. A., Kim, Y.-Y., Godinho, J. R. A., Kulak, A. N., Niño, C. G., Withers, P. J., et al. 2021. Exploiting Confinement to Study the Crystallization Pathway of Calcium Sulfate. *Advanced Functional Materials* 31: 2107312.

Armstrong, J. T., Meeker, G. P., Huneke, J. C., and Wasserburg, G. J. 1982. The Blue Angel: I. The Mineralogy and Petrogenesis of a Hibonite Inclusion from the Murchison Meteorite. *Geochimica et Cosmochimica Acta* 46: 575–95.

Ballirano, P., and Melis, E. 2009. Thermal Behaviour and Kinetics of Dehydration in Air of Bassanite, Calcium Sulphate Hemihydrate ($CaSO_4 \cdot 0.5H_2O$), from X-Ray Powder Diffraction. *European Journal of Mineralogy* 21: 985–93.

Barber, D. J. 1981. Matrix Phyllosilicates and Associated Minerals in C2M Carbonaceous Chondrites. *Geochimica et Cosmochimica Acta* 45: 945–70.

Bland, P. A., Zolensky, M. E., Benedix, M. E., and Sephton, M. A. 2006. Weathering of Chondritic Meteorites. In *Meteorites and the Early Solar System II*, edited by D. S. Lauretta and H. Y. McSween, Jr., 853–67. Tuscon, Arizona: The University of Arizona Press.

Botta, O., and Bada, J. L. 2002. Extraterrestrial Organic Compounds in Meteorites. *Surveys in Geophysics* 23: 411–67.

Brandstätter, F., Brack, A., Baglioni, P., Cockell, C. S., Demets, R., Edwards, H. G. M., Kurat, G., et al. 2008. Mineralogical Alteration of Artificial Meteorites During Atmospheric Entry. The STONE-5 Experiment. *Planetary and Space Science* 56: 976–84. https://doi.org/10.1016/j.pss.2007.12.014.

Brearley, A. J. 2006. The Action of Water. In *Meteorites and the Early Solar System II*, edited by D. S. Lauretta and H. Y. McSween, Jr., 587–624. Tuscon, Arizona: The University of Arizona Press.

Bunch, T. E., and Chang, S. 1980. Carbonaceous Chondrites—II. Carbonaceous Chondrite Phyllosilicates and Light Element Geochemistry as Indicators of Parent Body Processes and Surface Conditions. *Geochimica et Cosmochimica Acta* 44: 1543–77.

Caillahua, M. C., and Moura, F. J. 2018. Technical Feasibility for Use of FGD Gypsum as an Additive Setting Time Retarder for Portland Cement. *Journal of Materials Research and Technology* 7: 190–7.

Cronin, J. R., and Pizzarello, S. 1990. Aliphatic Hydrocarbons of the Murchison Meteorite. *Geochimica et Cosmochimica Acta* 54: 2859–68.

Daly, L., Suttle, M.D., Lee, M.R., Bridges, J., Hicks, L., Martin, P.-E., Floyd, C.J., et al. Submitted. Nano-Scale Heterogeneity in the Extent of Aqueous Alteration within the Lithologies of the Winchcombe CM Carbonaceous Chondrite. *Meteoritics & Planetary Science.*

Drouard, A., Gattacceca, J., Hutzler, A., Rochette, P., Baucher, R., Bourlès, D., ASTER Team, et al. 2019. The Meteorite Flux of the Past 2 m.y. Recorded in the Atacama Desert. *Geology* 47: 673–6.

Ebert, A., Rieke-Zapp, D., Herwegh, M., Ramseyer, K., Gnos, E., and Decrouez, D. 2009. Microstructures of Coarse-Grained Marbles, Analyzed Using a New Technique Based on the Bireflectance of Calcite. *Tectonophysics* 463: 175–84.

Fan, Y., Li, S. J., and Liu, S. 2020. The Mineralogy and Geochemistry of Shidian: A New Fall of CM Chondrite in China (Abstract #1234). 51st Lunar and Planetary Science Conference. CD-ROM.

Fanale, F. P., Li, Y.-H., De Carlo, E., Farley, C., Sharma, S. K., Horton, K., and Granahan, J. C. 2001. An Experimental Estimate of Europa's Ocean Composition Independent of Galileo Orbital Remote Sensing. *Journal of Geophysical Research* 106: 14595–600.

Floyd, C. J., and Lee, M. R. 2021. Rapid Calcite Dissolution in CM Carbonaceous Chondrites and its Implications (Abstract #1335). 52nd Lunar and Planetary Science Conference. CD-ROM.

Fuchs, L. H., Olsen, E., and Jensen, K. J. 1973. Mineralogy, Mineral-Chemistry, and Composition of the Murchison (C2) Meteorite. *Smithsonian Contributions to the Earth Sciences* 10: 1–39. https://doi.org/10.5479/si.00810274.10.1.

Galdenzi, S., and Maruoka, T. 2003. Gypsum Deposits in the Frasassi Caves, Central Italy. *Journal of Cave and Karst Studies* 65: 111–25.

Gattacceca, J., McCubbin, F. M., Grossman, J., Bouvier, A., Bullock, E., Aoudjehane, H. C., Debaille, V., et al. 2021. The Meteoritical Bulletin, No. 109. *Meteoritics & Planetary Science* 56: 1626–30.

Genge, M. J., Alesbrook, L., Almeida, N. V., Bates, H. C., Bland, P. A., Boyd, M. R., Burchell, M. J., et al. 2023. The Fusion Crust of the Winchcombe Meteorite: A Preserved Record of Atmospheric Entry Processes. *Meteoritics & Planetary Science*. Portico. https://doi.org/10.1111/maps.13937.

Genge, M. J., and Grady, M. M. 1999. The Fusion Crusts of Stony Meteorites: Implications for the Atmospheric Reprocessing of Extraterrestrial Materials. *Meteoritics & Planetary Science* 34: 341–56.

Gounelle, M., and Zolensky, M. E. 2001. A Terrestrial Origin for Sulfate Veins in CI1 Chondrites. *Meteoritics & Planetary Science* 36: 1321–9.

Gounelle, M., and Zolensky, M. E. 2014. The Orgueil Meteorite: 150 Years of History. *Meteoritics & Planetary Science* 49: 1769–94.

Gozzi, F., Gaeta, M., Freda, C., Mollo, S., Di Rocco, T., Marra, F., Dallai, L., and Pack, A. 2014. Primary Magmatic Calcite Reveals Origin from Crustal Carbonate. *Lithos* 190-191: 191–203.

Grossman, J. N. 2000. A Meteorite Falls on Ice. *Science* 290: 283–5.

Habermann, D., Neuser, R. D., and Richter, D. K. 1996. REE-Activated Cathodoluminescence of Calcite and Dolomite: High-Resolution Spectrometric Analysis of CL Emission (HRS-CL). *Sedimentary Geology* 101: 1–7.

Hajar, Y., McAuley, K., and Zeman, F. 2016. Sulfur as a Fuel Source in a Combined Power Cycle Equipped with a Dry Flue Gas Desulfurization System. *Energy & Fuels* 30: 8511–9.

Hardie, L. A., and Eugster, H. P. 1970. The Evolution of Closed-Basin Brines. *Mineralogical Society of America Special Papers* 3: 273–90.

Herd, C. D. K., Hilts, R. W., Skelhorn, A. W., and Simkus, D. N. 2016. Cold Curation of Pristine Astromaterials: Insights from the Tagish Lake Meteorite. *Meteoritics & Planetary Science* 51: 499–519.

Hezel, D. C., Poole, G. M., Hoyes, J., Coles, B. J., Unsworth, C., Albrecht, N., Smith, C., et al. 2015. Fe and O Isotope Composition of Meteorite Fusion Crusts: Possible Natural Analogues to Chondrule Formation? *Meteoritics & Planetary Science* 50: 229–42.

Hose, L. D., and Rosales-Lagarde, L. 2017. Sulfur-Rich Caves of Southern Tabasco, Mexico. In *Hypogene Karst Regions and Caves of the World. Cave and Karst Systems of the World*, edited by A. N. Klimchouk, A. Palmer, J. S. De Waele, A. Auler, and P. Audra. Cham: Springer.

Howard, K. T., Alexander, C. M. O'D., Schrader, D. L., and Dyl, K. A. 2015. Classification of Hydrous Meteorites (CR, CM and C2 Ungrouped) by Phyllosilicate Fraction: PSD-XRD Modal Mineralogy and Planetesimal Environments. *Geochimica et Cosmochimica Acta* 149: 206–22.

Ito, M., Tomioka, N., Uesugi, M., Yamaguchi, A., Shirai, N., Ohigashi, T., Liu, M. C., et al. 2022. A Pristine Record of Outer Solar System Materials from Asteroid Ryugu's Returned Sample. *Nature Astronomy* 6: 1163–71.

Ivanov, A. V., Yaroshevskiy, A. A., and Ivanova, M. A. 2019. Meteorite Minerals. *Geochemistry International* 57: 931–9.

Izawa, M. R. M., Nesbitt, H. W., MacRae, N. D., and Hoffman, E. L. 2010. Composition and Evolution of the Early Oceans: Evidence from the Tagish Lake Meteorite. *Earth and Planetary Science Letters* 298: 443–9.

Jenniskens, P., Fries, M. D., Yin, Q.-Z., Zolensky, M., Krot, A. N., Sandford, S. A., Sears, D., et al. 2012. Radar-Enabled Recovery of the Sutter's Mill Meteorite, a Carbonaceous Chondrite Regolith Breccia. *Science* 338: 1583–7.

Jull, A. J. T., Donahue, D. J., Cielazyk, E., and Wlotzka, F. 1993. Carbon-14 Terrestrial Ages and Weathering of 27 Meteorites from the Southern High Plains and Adjacent Areas (USA). *Meteoritics* 28: 188–95.

Kim, Y., Caumon, M.-C., Barres, O., Sall, A., and Cauzid, J. 2021. Identification and Composition of Carbonate Minerals of the Calcite Structure by Raman and Infrared Spectroscopies Using Portable Devices. *Spectrochimica Acta Part A: Molecular and Biomolecular Spectroscopy* 261: 119980.

King, A. J., Bates, H. C., Schofield, P. F., and Russell, S. S. 2021. The Bulk Mineralogy and Water Contents of the Carbonaceous Chondrite Falls Kolang and Tarda (Abstract #1909). 52nd Lunar and Planetary Science Conference. CD-ROM.

King, A. J., Daly, L., Rowe, J., Joy, K. H., Greenwood, R. C., Devillepoix, H. A. R., Suttle, M. D., et al. 2022. The Winchcombe Meteorite, a Unique and Pristine Witness from the Outer Solar System. *Science Advances* 8: eabq3925.

King, A. J., Phillips, K. J. H., Strekopytov, S. S., Vita-Frinzi, C., and Russell, S. S. 2020. Terrestrial Modification of the Ivuna Meteorite and a Reassessment of the Chemical Composition of the CI Type Specimen. *Geochimica et Cosmochimica Acta* 268: 73–89.

Kvenvolden, K., Lawless, J., Pering, K., Peterson, E., Flores, J., Ponnamperuma, C., Kaplan, I. R., and Moore, C. 1970. Evidence for Extraterrestrial Amino-Acids and Hydrocarbons in the Murchison Meteorite. *Nature* 228: 923–6.

Lauretta, D. S., Balram-Knutson, S. S., Beshore, E., Boynton, W. V., Drouet d'Aubigny, C., DellaGiustina, D. N., Enos, H. L., et al. 2017. OSIRIS-REx: Sample Return from Asteroid (101955) Bennu. *Space Science Reviews* 212: 925–84.

Lee, M. R. 1993. The Petrography, Mineralogy and Origins of Calcium Sulfate within the Cold Bokkeveld CM Carbonaceous Chondrite. *Meteoritics* 28: 53–62.

Lee, J. K. W. 1995. Multipath Diffusion in Geochronology. *Contributions to Mineralogy and Petrology* 120: 60–82. https://doi.org/10.1007/bf00311008.

Lee, M. R., and Bland, P. A. 2004. Mechanisms of Weathering of Meteorites Recovered from Hot and Cold Deserts and the Formation of Phyllosilicates. *Geochimica et Cosmochimica Acta* 68: 893–916.

Lee, M. R., Cohen, B. E., and King, A. J. 2019. Alkali-Halogen Metasomatism of the CM Carbonaceous Chondrites. *Meteoritics & Planetary Science* 54: 3052–63.

Lee, M. R., Daly, L., Floyd, C., and Martin, P.-E. 2021. CM Carbonaceous Chondrite Falls and their Terrestrial Alteration. *Meteoritics & Planetary Science* 56: 34–48.

Lee, M. R., Lindgren, P., and Sofe, M. R. 2014. Aragonite, Breunnerite, Calcite and Dolomite in CM Carbonaceous Chondrites: High Fidelity Recorders of Progressive Parent Body Aqueous Alteration. *Geochimica et Cosmochimica Acta* 144: 126–56.

Liu, Y., Wang, A., and Freeman, J. J. 2009. Raman, MIR, and NIR Spectroscopic Study of Calcium Sulfates: Gypsum, Bassanite, and Anhydrite (Abstract #2128). 40th Lunar and Planetary Science Conference. CD-ROM.

Losiak, A., and Velbel, M. A. 2011. Evaporite Formation during Weathering of Antarctic Meteorites—A Weathering Census Analysis Based on the ANSMET Database. *Meteoritics & Planetary Science* 46: 443–58.

Maclear, T. 1840. VIII. Further Particulars of the Fall of the Cold Bokkeveld Meteorolite. By Thomas Maclear, Esq. F.R.S. &c., in a Letter to Sir John F. W. Herschel, Bart. K. H. V. P. R. S. &c. &c. Communicated by Sir John F. W. Herschel. *Philosophical Transactions of the Royal Society* 130: 177–82.

Met Office Weather Observations Website. 2022. Observation Site Bishops Cleeve. Last modified May 16. https://wow.metoffice.gov.uk/observations/details/20210301o3j4kbd4sae6zd8pyyb96scn9y.

McMullan, S., Denis, V., Devillepoix, H., Daly, L., King, A., Cupak, M., Howie, R., et al. in review. The Winchcombe Fireball-that Lucky Survivor. *Meteoritics & Planetary Science*.

Nagao, K., Okazaki, R., Nakamura, T., Miura, Y. N., Osawa, T., Bajo, K.-I., Matsuda, S., et al. 2011. Irradiation History of Itokawa Regolith Material Deduced from Noble Gases in the Hayabusa Samples. *Science* 333: 1128–31.

Nakamuta, Y., Nakamura, T., and Nakamura, N. 2006. Structural State of Plagioclase from the Kobe CK Chondrite: Implications for the Thermal History of the CK Parent Body. *Journal of Mineralogical and Petrological Science* 101: 308–18.

Newman, E. S. 1941. Behavior of Calcium Sulfate at High Temperatures. *Journal of Research of the National Bureau of Standards* 27: 191–6.

Nittler, L. R., Stroud, R. M., Trigo-Rodríguez, J. M., De Gregorio, B. T., Alexander, C. M. O'D., Davidson, J., Moyano-Cambero, C. E., and Tanbakouei, S. 2019. A Cometary Building Block in a Primitive Asteroidal Meteorite. *Nature Astronomy* 3: 659–66.

Pirlet, H., Wehrmann, L. M., Brunner, B., Frank, N., Dewanckele, J., Van Rooij, D., Foubert, A., et al. 2010. Diagenetic Formation of Gypsum and Dolomite in a Cold-Water Coral Mound in the Porcupine Seabight, off Ireland. *Sedimentology* 57: 786–805.

Reddy, S. M., Saxey, D. W., Rickard, W. D. A., Fougerouse, D., Montalvo, S. D., Verberne, R., and van Riessen, A. 2020. Atom Probe Tomography: Development and Application to the Geosciences. *Geostandards and Geoanalytical Research* 44: 5–50.

Richter, D. K., Neuser, R. D., Harder, M., Schabdach, H., and Scholz, D. 2018. Unusual Internal Structure of cm-Sized Coldwater Calcite: Weichselian Spars in Former Pools of the Zinnbergschacht Cave (Franconian Alb/SE Germany). *International Journal of Speleology* 47: 145–54.

Riciputi, L. R., McSween, H. Y., Jr., Johnson, C. A., and Prinz, M. 1994. Minor and Race Element Concentrations in Carbonates of Carbonaceous Chondrites, and Implications for the Compositions of Co-Existing Fluids. *Geochimica et Cosmochimica Acta* 58: 1343–51.

Rubin, A. E. 1997. Mineralogy of Meteorite Groups. *Meteoritics & Planetary Science* 32: 231–47.

Rubin, A. E. 2015. An American on Paris: Extent of Aqueous Alteration of a CM Chondrite and the Petrography of its Refractory and Amoeboid Olivine Inclusions. *Meteoritics & Planetary Science* 50: 1595–612.

Rubin, A. E., Trigo-Rodríguez, J. M., Huber, H., and Wasson, J. T. 2007. Progressive Aqueous Alteration of CM Carbonaceous Chondrites. *Geochimica et Cosmochimica Acta* 71: 2361–82.

Russell, S. S., Salge, T., King, A., Daly, L., Joy, K., Bates, H., Almeida, N. V., Suttle, M., and Schofield, P. 2022. The Winchcombe CM2 Meteorite Fall: Curation and Preliminary Analysis. *Microscopy and Microanalysis* 28: 2732–3. https://doi.org/10.1017/s1431927622010273.

Saha, A., Lee, J., Pancera, S. M., Bräeu, M. F., Kempter, A., Tripathi, A., and Bose, A. 2012. New Insights into the Transformation of Calcium Sulfate Hemihydrate to Gypsum Using Time-Resolved Cryogenic Transmission Electron Microscopy. *Langmuir* 28: 11182–7.

Schrader, D. L., Connolly, H. C., Jr., Lauretta, D. S., Zega, T. J., Davidson, J., and Domanik, K. J. 2015. The Formation and Alteration of the Renazzo-Like Carbonaceous Chondrites III: Toward Understanding the Genesis of Ferromagnesian Chondrules. *Meteoritics & Planetary Sciences* 50: 15–50.

Strydom, C. A., Hudson-Lamb, D. L., Potgieter, J. H., and Dagg, E. 1995. The Thermal Dehydration of Synthetic Gypsum. *Thermochimica Acta* 269: 631–8.

Suttle, M. D., Daly, L., Jones, R. H., Jenkins, L., Van Ginneken, M., Mitchell, J. T., Bridges, J. C., et al. 2022. The Winchcombe Meteorite—A Regolith Breccia from a Rubble Pile CM Chondrite Asteroid. *Meteoritics &*

Planetary Science. Portico. https://doi.org/10.1111/maps. 13938.

Trigo-Rodríguez, J. M., Rimola, A., Tanbakouei, S., Soto, V. C., and Lee, M. 2019. Accretion of Water in Carbonaceous Chondrites: Current Evidence and Implications for the Delivery of Water to Early Earth. *Space Science Reviews* 215: 18.

Tritschler, U., Van Driessche, A. E. S., Kempter, A., Kellermeier, M., and Cölfen, H. 2015. Controlling the Selective Formation of Calcium Sulfate Polymorphs at Room Temperature. *Angewandte Chemie International Edition* 54: 4083–6. https://doi.org/10.1002/anie. 201409651.

Tyra, M. A., Farquhar, J., Wing, B. A., Benedix, G. K., Jull, A. J. T., Jackson, T., and Thiemens, M. H. 2007. Terrestrial Alteration of Carbonate in a Suite of Antarctic CM Chondrites: Evidence from Oxygen and Carbon Isotopes. *Geochimica et Cosmochimica Acta* 71: 782–95.

Van Schmus, W. R., and Wood, J. A. 1967. A Chemical-Petrologic Classification for Chondritic Meteorites. *Geochimica et Cosmochimica Acta* 31: 747–65.

Watanabe, S.-I., Tsuda, Y., Yoshikawa, M., Tanaka, S., Saiki, T., and Nakazawa, S. 2017. Hayabusa2 Mission Overview. *Space Science Reviews* 208: 3–16.

Yokoyama, T., Nagashima, K., Nakai, I., Young, E. D., Abe, Y., Aléon, J., Alexander, C. M. O'D., et al. 2022. Samples Returned from the Asteroid Ryugu Are Similar to Ivuna-Type Carbonaceous Meteorites. *Science* 376: 1–17.

Zurfluh, F. J., Hofmann, B. A., Gnos, E., and Eggenberger, U. 2013. "Sweating Meteorites"—Water-Soluble Salts and Temperature Variation in Ordinary Chondrites and Soil from the Hot Desert of Oman. *Meteoritics & Planetary Science* 48: 1958–80.